

# Structures of Au/Pt bimetallic clusters: homogeneous or segregated?

Fang Wang · Peng Liu · Dongju Zhang

Received: 23 November 2009 / Accepted: 16 July 2010 / Published online: 28 July 2010  
© Springer-Verlag 2010

**Abstract** The question whether Au can alloy with Pt at the nano-scale size is still controversial. By performing density functional theory calculations for several small Au/Pt bimetallic clusters  $\text{Au}_m\text{Pt}_n$  ( $m+n=4\text{--}6, 13$ ), we find that, in all the most stable geometries, Pt atoms prefer to assemble together to form the core while Au atoms like to surround the Pt atoms to form the shell, and that evenly mixed clusters are structurally unstable. The unique geometric characteristics can be explained by analyzing the different electronic properties of Pt–Pt, Au–Pt and Au–Au bonds, and is expected also to apply to larger Au/Pt bimetallic clusters.

**Keywords** Density functional theory · Au/Pt bimetallic clusters · Core-shell-like structure · Bonding nature

## Introduction

Au/Pt bimetallic nanoparticles (NPs) have attracted considerable attention in recent years [1, 2] due to their enhanced catalytic activity and durability in many important reactions, such as methanol and formic acid oxidations [3, 4] and oxygen reduction reactions [5], where Au/Pt bimetallic NPs act as the anode and cathode materials, respectively.

**Electronic supplementary material** The online version of this article (doi:10.1007/s00894-010-0815-4) contains supplementary material, which is available to authorized users.

F. Wang · P. Liu · D. Zhang (✉)  
School of Chemistry and Chemical Engineering,  
Shandong University,  
Jinan 250100, People's Republic of China  
e-mail: zhangdj@sdu.edu.cn

Au/Pt bimetallic NPs also show great promise in the field of fuel cell technology. To date, several Au/Pt bimetallic NPs with different composition, size, structure and morphology have been prepared successfully.

It is well known that a miscibility gap exists in bulk Au/Pt bimetallic systems over a wide Pt composition range (15–98%), with Au preferring to separate from the surface owing to its lower surface energy [6]. Regarding the miscibility of nano-scaled Au/Pt bimetallic particles, different reports show distinct results. Some groups have reported that Au/Pt NPs exhibit alloy properties [7, 8], while the others found that Au tends to migrate to the surface, covering active Pt sites [9, 10]. Such contrasting results indicate that the atomic ordering in nano-scaled Au/Pt bimetallic particles, which greatly influences the catalytic activity of NPs [11], is a complex issue that is still not well understood. Therefore, it is worthwhile to ascertain the stable atomic ordering of Au/Pt NPs theoretically.

In the present work, our attention focused on several small possible Au/Pt bimetallic clusters,  $\text{Au}_m\text{Pt}_n$  ( $m+n=4\text{--}6, 13$ ). By performing density functional theory (DFT) calculations, we studied their geometric and electronic structures to explore the stable atomic ordering of Au/Pt NPs at the small atomic sizes. It should be noted that the similar DFT calculations by Song et al. [12] and Tian et al. [13], as well as classical molecular dynamics (MD) simulations by Liu et al. [2, 14] have been published previously. However, the issues about atomic ordering was not discussed clearly. Our present calculations aim to provide insight into the geometric and electronic structures of Au/Pt bimetallic clusters at the atomic level. Based on the calculated results, we expect to gain a better understanding for the structures of Au/Pt bimetallic clusters.

## Computational details

The Gaussian 03 program package [15] was employed for all calculations in this study. The Perdew-Wang 91 exchange and correlation functional (commonly referred to as PW91) [16] was chosen based on its excellent performance in describing Au clusters [17]. Considering the strong relativistic effect of Au and Pt, the Los Alamos LANL2DZ effective core pseudopotentials (ECP) and valence double zeta basis sets were used for Au and Pt atoms [18]. No symmetric constraints were imposed during geometrical optimizations. Energy minima were identified by subsequent frequency calculations, which also provided zero-point vibrational energy (ZPE) corrections. Natural bond orbital (NBO) analysis was performed to reveal the nature of Au–Pt, Au–Au and Pt–Pt bonds.

To ascertain the accuracy of the chosen functional and ECP, we performed benchmark calculations of electron affinities (EAs) and ionization energies (IEs) for  $\text{Au}_m$  ( $m=4\text{--}6$ ) and  $\text{Pt}_n$  ( $n=3\text{--}4$ ) clusters. As shown in Table 1, the theoretical EA and IE values are in fairly good agreement with the corresponding experimental results [19–21]. In addition, the calculated bond dissociation energy of  $\text{Au}_2$  (2.19 eV) is also consistent with known experimental findings (2.29 eV). These facts indicate the acceptable accuracy and reliability of the PW91/LANL2DZ method for describing small bimetallic Au–Pt clusters.

## Results and discussion

### Geometries of $\text{Au}_m\text{Pt}_n$ ( $m+n=4\text{--}6$ ) clusters

For comparison, we first calculated the ground state structures of pure  $\text{Au}_m$  and  $\text{Pt}_n$  ( $m, n=4\text{--}6$ ). As can be seen in Fig. 1, the energetically most favorable structures

**Table 1** Calculated and experimental electron affinities (EAs) and ionization energies (IEs) of  $\text{Au}_m$  ( $m=4\text{--}6$ ) and  $\text{Pt}_n$  ( $n=3\text{--}4$ ); energies are in eV

Species	Calculated		Experimental	
	EA	IE	EA	IE
$\text{Au}_4$	2.84	8.26	$2.60\pm 0.1^{\text{a}}$	8.59 <sup>b</sup>
$\text{Au}_5$	3.26	7.58	$2.93\pm 0.1^{\text{a}}$	$7.61\pm 0.02^{\text{c}}$
$\text{Au}_6$	2.31	8.41	$2.051\pm 0.002^{\text{a}}$	...
$\text{Pt}_3$	2.11	8.12	$1.87\pm 0.02^{\text{a}}$	...
$\text{Pt}_4$	2.10	6.89	...	...

<sup>a</sup>[19]

<sup>b</sup>[20]

<sup>c</sup>[21]

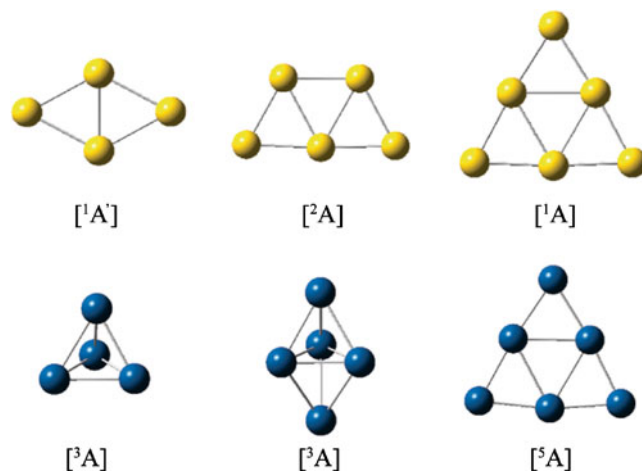


**Fig. 1** Optimized geometries of pure  $\text{Au}_m$  ( $m=4\text{--}6$ ) and  $\text{Pt}_n$  ( $n=4\text{--}6$ ) clusters. The gold and blue balls denote Au and Pt atoms, respectively. The values in square brackets are electronic states of the clusters

for all three pure gold clusters have a two-dimensional (2D) characteristic, and this geometrical characteristic is also true for  $\text{Pt}_6$ . However, for  $\text{Pt}_4$  and  $\text{Pt}_5$ , our calculations show that three-dimensional (3D) structures are more favorable in energy than planar configurations. The tetrahedral  $\text{Pt}_4$  and trigonal bipyramidal  $\text{Pt}_5$  are calculated to be 0.30 and 0.18 eV more stable than the most stable 2D structures, respectively.

The ground state geometries of  $\text{Au}_m\text{Pt}_n$  ( $m+n=4\text{--}6$ ) bimetallic clusters are presented in Fig. 2. As can be seen, most of the clusters are planar ( $\text{Au}_5\text{Pt}$ ,  $\text{Au}_4\text{Pt}_2$  and  $\text{AuPt}_5$ ) or quasi-planar, except  $\text{AuPt}_3$  and  $\text{AuPt}_4$ . For the four-atom bimetallic clusters, there are three possible composition combinations, i.e.,  $\text{Au}_3\text{Pt}$ ,  $\text{Au}_2\text{Pt}_2$ , and  $\text{AuPt}_3$ . Similarly, there are four and five possible composition combinations for the five- and six-atom clusters, respectively. We next analyzed the geometrical characteristics of these clusters one by one.

When an atom of  $\text{Au}_4$  is replaced by Pt, the Pt atom prefers to substitute the Au atom with the highest coordination numbers, i.e., 1-site Au or 4-site Au to form  $\text{Au}_3\text{Pt}$  shown in Fig. 2. For  $\text{Au}_2\text{Pt}_2$ , the geometry with two Pt atoms located at the 1-site and 4-site is the most stable, where two Au atoms stay away from each other to form Au–Pt bonds as many as possible. This configuration is energetically 0.49 eV more stable than the most stable 3D structure, which has a tetrahedral shape (see  $\text{Au}_2\text{Pt}_2$  in Fig. S1 in the electronic supplementary material). In the case of  $\text{AuPt}_3$ , three Pt atoms form a “core”, and the Au atom coordinates to this core to give a tetrahedral structure.

For the five-atom bimetallic clusters, possible composition combinations are  $\text{Au}_4\text{Pt}$ ,  $\text{Au}_3\text{Pt}_2$ ,  $\text{Au}_2\text{Pt}_3$ ,  $\text{Au}_3\text{Pt}_2$ , and  $\text{Au}_4\text{Pt}$ . In the most stable geometry of  $\text{Au}_4\text{Pt}$ , the Pt possesses a larger coordination number compared with Au atoms. This geometrical characteristic is consistent with that

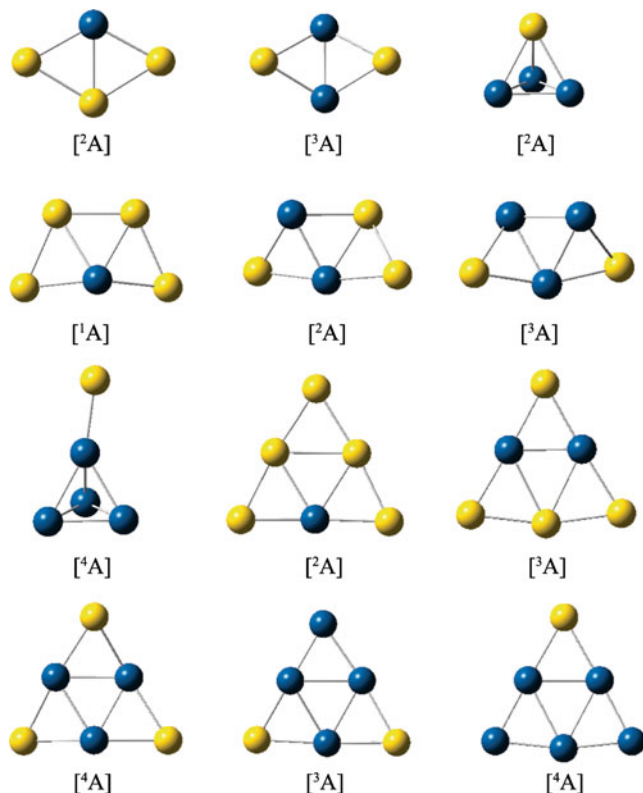


**Fig. 2** Optimized geometries of  $\text{Au}_m\text{Pt}_n$  ( $m+n=4-6$ ) bimetallic clusters. The gold and blue balls denote Au and Pt atoms, respectively. The values in square brackets are electronic states of the clusters

of  $\text{Au}_3\text{Pt}$ . It is worth noting that the trigonal bipyramidal  $\text{Au}_4\text{Pt}$ , with the Pt atom located at the shared surface (see **Au<sub>4</sub>Pt-1** in Fig. S1) is comparable in energy with the ground state structure. In the ground state geometry of  $\text{Au}_3\text{Pt}_2$ , two Pt atoms abut each other, and three Au atoms are located next to the two sides of the Pt atoms. Similarly, in  $\text{Au}_2\text{Pt}_3$  and  $\text{AuPt}_4$ , Pt atoms prefer to form the cores and Au atoms tend to distribute around the core. For the  $\text{AuPt}_4$  cluster, we also located another low-energy geometry with the Au atom localized adjacent to the tetrahedron wall (see **AuPt<sub>4</sub>-2** in Fig. S1), which is calculated to be less stable by 0.26 eV than the ground state structure.

The observed geometrical characteristic described above also applied to six-atom bimetallic clusters, that is, Pt atoms tend to form a core and Au atoms prefer to locate in sites with low coordination numbers and to surround the Pt atoms to form a shell. This characteristic is clear from the geometries shown in Fig. 2. Additionally, it is found that all the geometries for six-atom bimetallic clusters are planar or quasi-planar. Note that the configuration of  $\text{Au}_2\text{Pt}_4$  is not simply an extension of that of  $\text{AuPt}_4$ , indicating compositions of the Au–Pt clusters determinately effect their geometries. We have also calculated the most stable 3D configuration for  $\text{Au}_2\text{Pt}_4$  (see **Au<sub>2</sub>Pt<sub>4</sub>-1** in Fig. S1). It is less stable by 0.24 eV in energy than its ground planar geometry.

In addition, the geometries of Au/Pt bimetallic clusters were found to match the low-lying energy geometries of monometallic clusters, that is, the geometries of the binary clusters resemble those of the pure metal clusters, the composition of which is larger in binary clusters. For example,  $\text{AuPt}_3$  presents a tetrahedral geometry, which is similar to that of  $\text{Pt}_4$ , due to the fact that Pt in the cluster is larger than Au. A similar trend was also found by Lee et al. [22] for Au/Ag binary clusters.

To sum up, in the small  $\text{Au}_m\text{Pt}_n$  ( $m+n=4-6$ ) bimetallic clusters, Pt atoms tend to hold the sites with the highest coordination numbers and aggregate together to form the center of Au/Pt bimetallic clusters, while Au atoms prefer to locate in sites with lower coordination numbers, and to spread around the Pt atoms.

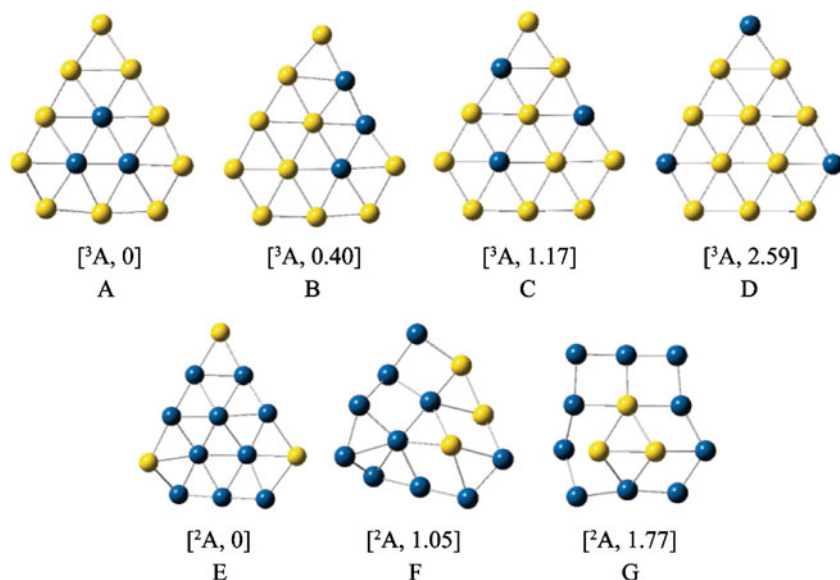
#### Geometries of $\text{Au}_m\text{Pt}_n$ ( $m+n=13$ , and $m=3$ or 10) clusters

To verify whether the geometric characteristics of the small Au/Pt bimetallic clusters also apply to larger clusters, we investigated the geometries of two larger planar clusters,  $\text{Au}_{10}\text{Pt}_3$  and  $\text{Au}_3\text{Pt}_{10}$ . To determine global minimum is extremely difficult, and computational limits usually preclude such claims for medium-sized clusters. Here, we restricted our calculations to several planar cluster configurations for these two larger clusters. Although they may not be the most stable geometries of  $\text{Au}_{10}\text{Pt}_3$  and  $\text{Au}_3\text{Pt}_{10}$  clusters, the calculated relative stability of these clusters provided enough information for our purposes in the present study. The optimized geometries are shown in Fig. 3. For  $\text{Au}_{10}\text{Pt}_3$ , among the four chosen configurations, structure **A** with three Pt atoms placed at the center is the most stable, being more stable in energy by 0.40, 1.17, and 2.59 eV than structures **B**, **C**, and **D**, where the three Pt atoms are partly or completely separated by Au atoms. Similarly, for  $\text{Au}_3\text{Pt}_{10}$ , structure **E**, where Pt atoms concentrate at the center and Au atoms locate at the vertexes, was the most stable. This structure is calculated to be 1.05 and 1.77 eV more stable in energy than structures **F** and **G**, respectively, where three Au rather than Pt atoms are adjacent to each other. Clearly, the geometrical characteristic of the most stable  $\text{Au}_{10}\text{Pt}_3$  and  $\text{Au}_3\text{Pt}_{10}$  among the chosen configurations can also be described by a so-called Pt-core-Au-shell structure, confirming that the geometrical characteristic found for the smaller Au/Pt bimetallic clusters also applies to these medium-sized Au/Pt bimetallic clusters.

#### Electronic properties of $\text{Au}_m\text{Pt}_n$ ( $m+n=4-6$ , 13) clusters

Why do Au/Pt bimetallic clusters prefer to form core-shell-like structures? We have attempted to explain this by their electronic properties. NBO analysis revealed that Pt–Pt, Pt–

**Fig. 3** Optimized geometries of  $\text{Au}_{10}\text{Pt}_3$  and  $\text{Au}_3\text{Pt}_{10}$  clusters. The gold and blue balls denote Au and Pt atoms, respectively. The symbols and values in square brackets denote the electronic states and the relative energies (in eV) with respect to the most stable structure



Au, and Au–Au bonds differ intrinsically in nature. As an example, in Table 2 we show the hybrid orbital composition of Pt–Pt, Pt–Au, and Au–Au bonds in the  $\text{Au}_3\text{Pt}_2$  cluster. Clearly, the Pt–Pt bond is formed mainly through the overlap of *s-d* hybridized orbitals of two Pt atoms, the Pt–Au bond originates primarily from the overlap of the *s-d* hybridized orbital of Pt with the *6s* orbital of Au, while for the Au–Au bond, the overlap of *6s* orbitals between the two Au atoms makes a major contribution. These bonding characteristics are also true in all other bimetallic clusters that have been studied. Generally, hybridized orbitals are beneficial to the maximum overlap between atomic orbitals, that is, the bonding capability of hybridized atomic orbitals is much stronger than that of non-hybridized atomic orbitals. Thus, the bond formed by the overlap of hybrid orbitals is much more stable than that formed by non-hybridized atomic orbitals. Therefore the bond strength of Pt–Pt, Pt–Au, and Au–Au bonds is expected to follow the trend: Pt–Pt > Au–Pt > Au–Au. In order to verify this conjecture, we have calculated the bond dissociation energies ( $E_b$ ) of Pt–Pt, Pt–Au, and Au–Au bonds for the three dimers  $\text{Pt}_2$ ,  $\text{AuPt}$  and  $\text{Au}_2$ . The  $E_b$  value of  $\text{Pt}_2$

(3.53 eV) was found to be largest, followed by that of  $\text{AuPt}$  (2.43 eV), with the  $E_b$  value of  $\text{Au}_2$  (2.19 eV) smallest. This result confirms the bond strength order of Pt–Pt > Au–Pt > Au–Au. The strongest interaction among Pt atoms dictates the mixture of Pt and Au atoms prior to formation of the Pt–Pt core, and then Au interacts with this Pt–core to form the shell. The Pt–core–Au–shell structures so formed are the most favorable in energy.

From the results above, it is clear that Pt–core–Au–shell-like structures are the energetically most favorable form for Au/Pt bimetallic clusters, which is consistent with a recent report of classical MD simulations for Au–Pt NPs [2]. This fact implies that the phase-separation in nano-sized Au–Pt bimetallic structures could represent a spontaneous behavior. In other words, the very considerable miscibility gap in the bulk Pt–Au phase diagram [23–25] might have a great influence on the structural characteristics of their NPs.

## Conclusions

The geometric and electronic structures of the small  $\text{Au}_m\text{Pt}_n$  ( $m+n=4–6, 13$ ) bimetallic clusters have been investigated by performing DFT calculations. It was found that Au and Pt atoms prefer to form a core–shell-like structure, with Pt atoms assembling together to form the core and Au atoms surrounding the Pt atoms forming the shell. Evenly mixed clusters were found to be structurally unstable; this is attributed to the distinct nature of Pt–Pt, Pt–Au, and Au–Au bonds. The present study provides atomic-level insight into the geometric and electronic structure of Au/Pt bimetallic clusters, which can aid our understanding of the microstructure of Au/Pt bimetallic nanomaterials.

**Table 2** Natural bond orbital (NBO) analysis of hybrid orbital composition for  $\text{Au}_3\text{Pt}_2$  clusters

Bond	Hybrid composition
Pt3–Pt5	$0.6910(\text{sd}^{2.06})_{\text{Pt}} + 0.7229(\text{sd}^{2.13})_{\text{Pt}}$
Pt3–Au2	$0.6631(\text{sd}^{0.69})_{\text{Pt}} + 0.7485(\text{s})_{\text{Au}}$
Au1–Pt5	$0.7686(\text{s})_{\text{Au}} + 0.6397(\text{sd}^{0.57})_{\text{Pt}}$
Pt3–Au2	$0.5770(\text{s})_{\text{Pt}} + 0.8167(\text{s})_{\text{Au}}$
Au1–Au4	$0.7787(\text{s})_{\text{Au}} + 0.6274(\text{s})_{\text{Au}}$

**Acknowledgments** This work was sponsored by the National Science Foundation of China (20873076, 20773078), and the Specialized Research Fund for the Doctoral Program of Higher Education (No. 200804220009).

## References

1. Zhang J, Sasaki K, Sutter E, Adzic RR (2007) *Science* 315:220–222
2. Liu HB, Pal U, Ascencio JA (2008) *J Phys Chem C* 112:19173–19177
3. Zhang JT, Ma HY, Zhang DJ, Liu PP, Tian F, Ding Y (2008) *Phys Chem Chem Phys* 10:3250–3255
4. Peng ZM, Yang H (2009) *Nano Res* 2:406–415
5. Hernández-Fernández P, Rojas S, Ocón P, de la Gómez Fuente JL, San Fabián J, Sanza J, Peña MA, García-García FJ, Terreros P, Fierro JLG (2007) *J Phys Chem C* 111:2913–2923
6. Okamoto H, Massalski TB (1985) *Bull Alloy Phase Diagr* 6:46–56
7. Luo J, Maye MM, Petkov V, Kariuki NN, Wang L, Njoki P, Mott D, Lin Y, Zhong CJ (2005) *Chem Mater* 17:3086–3091
8. Mihut C, Descorme C, Duprez D, Amiridis MD (2002) *J Catal* 212:125–135
9. Selvarani G, Vinod Selvaganesh S, Krishnamurthy S, Kiruthika GVM, Sridhar P, Pitchumani S, Shukla AK (2009) *J Phys Chem C* 113:7461–7468
10. Abrams BL, Vesborg PCK, Bonde JL, Jaramillo TF, Chorkendorff I (2009) *J Electrochem Soc* 156:B273–B282
11. Chen F, Johnston RL (2008) *Acta Mater* 56:2374–2380
12. Song C, Ge Q, Wang L (2005) *J Phys Chem B* 109:22341–22350
13. Tian W, Ge M, Gu F, Yamada T, Aoki Y (2006) *J Phys Chem A* 110:6285–6293
14. Mariscal MM, Dassie SA, Leiva EPM (2005) *J Chem Phys* 123:184505
15. Frisch MJ, Trucks GW, Schlegel HB, Scuseria GE, Robb MA, Cheeseman JR, Montgomery JA Jr, Vreven T, Kudin KN, Burant JC, Millan JM, Iyengar SS, Tomasi J, Barone V, Mennucci B, Cossi M, Scalmani G, Rega N, Petersson GA, Nakatsuji H, Hada M, Ehara M, Toyota K, Fukuda R, Hasegawa J, Ishida M, Nakajima T, Honda Y, Kitao O, Nakai H, Klene M, Li X, Knox JE, Hratchian HP, Cross JB, Adamo C, Jaramillo J, Gomperts R, Stratmann RE, Yazyev O, Austin AJ, Cammi R, Pomelli C, Ochterski JW, Ayala PY, Morokuma K, Voth GA, Salvador P, Dannenberg JJ, Zakrzewski VG, Dapprich S, Daniels AD, Strain MC, Farkas O, Malick DK, Rabuck AD, Raghavachari K, Foresman JB, Ortiz JV, Cui Q, Baboul AG, Clifford S, Cioslowski J, Stefanov BB, Liu G, Liashenko A, Piskorz P, Komaromi I, Martin RL, Fox DJ, Keith T, Al-Laham MA, Peng CY, Nanayakkara A, Challacombe M, Gill PMW, Johnson B, Chen W, Wong MW, Gonzalez C, Pople JA (2004) Gaussian 03, Revision D.01. Gaussian Inc, Wallingford, CT
16. Burke K, Perdew JP, Wang Y (1998) Electronic density functional theory: recent progress and new directions. Plenum, New York
17. Walker AV (2005) *J Chem Phys* 122:094310
18. Hay PJ, Wadt WR (1985) *J Chem Phys* 82:270–283
19. Rienstra-Kiracofe JC, Tschumper GS, Schaefer HFIII, Nandi S, Ellison GB (2002) *Chem Rev* 102:231–282
20. Jackslath C, Rabin I, Schulze W (1992) *Ber Bunsenges Phys Chem* 96:1200–1204
21. Cheeseman MA, Eyler JR (1992) *J Phys Chem* 96:1082–1087
22. Lee HM, Ge M, Sahu BR, Tarakeshwar P, Kim KS (2003) *J Phys Chem B* 107:9994–10005
23. Massalski TB, Okamoto H, Subramanian PR, Kacprzak L (1990) Binary alloy phase diagrams. American Society of Metals, Materials Park
24. Porter A, Easterling KE (1992) Phase transformations in metals and alloys. Chapman and Hall, London
25. Ponec V, Bond GC (1995) Catalysis by metals and alloys, studies in surface science and catalysis, vol 95. Elsevier, Amsterdam